Proposal for J-PARC 50 GeV Proton Synchrotron

Study on Λ-Hypernuclei with the Charge-Exchange Reactions

S. Ajimura, A. Sakaguchi[1] , T. Kishimoto,
Osaka University, Toyonaka, Osaka 560-0043, Japan

H. Noumi, T. Takahashi,
High Energy Accelerator Research Organization (KEK), Tsukuba, Ibaraki 305-0801, Japan

T. Fukuda, Y. Mizoi,
Osaka Electro-communications University, Neyagawa, Osaka 572-8530, Japan

H. Outa,
Institute of Physical and Chemical Research (RIKEN), Wako, Saitama 351-0198, Japan

H. Bhang,
Seoul National University, Seoul 151-742, Korea

P.K. Saha,
Japan Atomic energy Agency (JAEA), Tokai, Ibaraki 319-1195, Japan

L. Busso,
Università di Torino, I-10125 Torino, Italy

D. Faso,
INFN, Sezione di Torino, I-10125 Torino, Italy

and

O. Morra
INAF-IFSI, Sezione di Torino, C.so Fiume 4, I-10125 Torino, Italy

28 April, 2006

Abstract

We propose to study the strong ΛN and weak ΛN interaction in the Λ hypernuclei by using the charge-exchange (CX) reactions, the (π^-, K^0) and (π^-, K^+) reactions, together with the ordinary strangeness exchange reactions, the (π^+, K^+) and (K^-, π^-) reactions. The new spectroscopic tool may open doors to new fields of hypernuclear physics, such as systematic studies on the neutron-rich and exotic Λ hypernuclei and detailed studies on the weak ΛN interaction. We will take two step approach, "phase 1" and "phase 2". The "phase 1" experiments are feasible with infrastructures available at the Day-1, and the "phase 2" experiments require a development and a construction of the high-intensity and high-resolution (HIHR) beamline and spectrometer system.

[1] Spokesperson, e-mail: sakaguch@phys.sci.osaka-u.ac.jp, phone: +81-6-6850-5352.

1 Introduction

The Λ-hypernucleus was identified experimentally for the first time in 1953 in a nuclear emulsion exposed to cosmic rays[1]. Since then, number of experiments have been carried out, innovative methods/techniques have been developed and many aspects of the Λ-hypernuclei have become clear. As a J-PARC experimental proposal by using the slow-extraction secondary beamline, we propose new innovative methods to study the new field of the hypernuclear physics. Key techniques for the studies are the development of *the charge exchange (CX) reactions*, which exchange charges or non-zero isospin together with the strangeness, and the construction of *high-intensity and high-resolution (HIHR) beamline and kaon spectrometer system* suitable and powerful for the study. The combination of the CX reactions and the HIHR beamline makes us possible to produce neutron-rich Λ hypernuclei and study the non-mesonic weak decays of Λ hypernuclei in detail.

1.1 Status of study on Λ-hypernuclei

Before describing our experimental proposal at J-PARC, we summarize current status of the study on the Λ-hypernuclei in this section.

The similarity of the Λ hyperon with nucleons is one of key properties which brings the rich spectra of the Λ-hypernuclei. The ΛN attractive interaction is strong enough to create huge number of particle-stable Λ-hypernuclei. The Λ hyperon behaves like the 3rd "nucleon" in a core nucleus and Λ single-particle like states coupled to the core nucleus states are clearly observed in the hypernuclear level structures[2, 3]. The bulk properties of the Λ-nucleus interaction have been known and also the details of the interaction, the spin-dependent interaction, have been investigated from the early stage of the experimental studies at CERN-PS and BNL-AGS[4, 5, 6] because it has been well known that the spin-dependent interaction played an important role in the ordinary nuclei.

Significant progresses were made on the study of the spin-dependent Λ-nucleus interaction after the end of 1990's. A small but finite value of the spin-orbit Λ-nucleus interaction was determined for the first time from the BNL-AGS experiment by the γ-ray spectroscopy with NaI(Tl) detectors in 1998[7]. Another epoch-making progress was the success of the γ-ray spectroscopy with germanium detectors at KEK-PS and BNL-AGS in 1998, and values of the spin-dependent interactions, including spin-spin, spin-orbit and tensor interactions, became clear after a series of experiments[8, 9]. The hypernuclear level structure and the spin-dependent interactions in hypernuclei obtained from these experiments give essential information on the underlying ΛN interaction. So, studies on the strong interaction between a Λ hyperon and a nucleon have entered to a new era.

The Λ-hypernuclei is also promising as a playground of studies on the baryon-baryon weak interaction. The weak interaction at hadronic level was studied mainly in the decay of mesons and baryons, e.g., decays of kaons and hyperons. In the weak decay of the Λ-hypernuclei, a new mode, the $\Lambda N \to NN$ mode, of the weak interaction also contributes to. The decay process is known as the non-mesonic weak decay (NMWD) process together with the process of the simple hyperon decay in the nuclear medium, the mesonic weak decay (MWD). Block and Dalitz discussed the NMWD process with a phenomenological model, and pointed out that experimental data may provide information on the spin and isospin structures of the ΛN weak interaction[10]. Detailed experimental studies on the NMWD process started at BNL-AGS[11, 12] and very precise data became available from a series of experiments at KEK-PS[13, 14, 15, 16], which include branching ratios, decay widths and spin observables.

The NMWD process has been discussed with theoretical models based on the meson-exchange picture and also models based on the quark-cluster exchange[17, 18]. The theoretical models succeeded to reproduce a part of the experimental data.

Although the studies on the Λ-hypernuclei had considerable progresses in recent years as we discussed, still there are essential questions and problems to be investigated and solved experimentally. We discuss the subjects should be addressed in the following sections.

1.2 Study on ΛN strong interaction

At first, we make discussion on open issues related to the strong interaction between Λ hyperon and nucleon.

As we mentioned above, the ΛN interaction is attractive and the addition of the Λ-hyperon into a nucleus increases the total binding energy, so we expect the "hypernuclear table-of-isotopes" is even richer than the "table-of-isotopes" of the ordinary nuclei. On the other hand, up to now, we surveyed only a small fraction of hypernuclei in the hypernuclear table-of-isotopes. One of main reasons of the limited survey is that we mainly used (K^-, π^-) and (π^+, K^+) reactions to produce the Λ-hypernuclei. To survey wider area of the hypernuclear table-of-isotopes, we need new spectroscopic tools.

A pilot experiment to produce Λ-hypernuclei away from the stability-line was performed at KEK-PS by using the $(K^-_{Stopped}, \pi^+)$ reaction[19]. Starting from ordinary nuclear targets, the double charge-exchange (DCX) reaction may produce neutron-rich Λ-hypernuclei. In the KEK-PS experiment, only upper limits were obtained for the production rates of the neutron-rich Λ-hypernuclei due to tiny branching ratios to the DCX channel and a huge background from the in-flight decay process of Σ^+, $\Sigma^+ \to n\pi^+$. An improved study with the $(K^-_{Stopped}, \pi^+)$ reaction is in progress by the FINUDA collaboration at Frascati-DAΦNE[20], but the clear identification of the production of the neutron-rich hypernuclei was not accomplished, yet.

Another promising DCX reaction to produce and investigate the neutron-rich hypernuclei is the (π^-, K^+) reaction. A neutron-rich hypernucleus, ${}^{10}_{\Lambda}$Li, was attempted to produce at KEK-PS by the (π^-, K^+) reaction for the first time[21]. In the experiment, clear signal events were observed in the Λ bound region in the excitation energy spectrum of the hypernucleus as shown in Fig.1. Although the production cross section of the ${}^{10}_{\Lambda}$Li hypernucleus was estimated to be very small ($\sim$10nb/sr), roughly 10^{-3} of that of the (π^+, K^+) reaction (10 μb/sr, typically), the experimental data may provide completely new information on the structure of the Λ-hypernuclei with a large number of excess neutrons (${}^{10}_{\Lambda}$Li consists of 3 proton, 6 neutron and a Λ hyperon). Compared with the $(K^-_{Stopped}, \pi^+)$ reaction, the (π^-, K^+) reaction is almost background free at the Λ bound region (see the $-B_\Lambda <$ -20MeV region in Fig.1). The production of the neutron-rich hypernuclei with the (π^-, K^+) reaction may open doors to new fields of study as follows:

1. The systematic study on the neutron-rich Λ-hypernuclei may be possible. The structure change of the core nucleus is observed in the ${}^{7}_{\Lambda}$Li hypernucleus[22]. We may expect much larger structure changes of the core nuclei for the neutron-rich hypernuclei, and a systematic study on such effects may be possible. The neutron-rich hypernuclei also include very exotic objects like ${}^{6}_{\Lambda}$H, bound state of p+4n+Λ, or even ${}^{7}_{\Lambda}$H, p+5n+Λ.

2. We may fill up the S(strangeness)=-1 sector and reveal several new phenomena of the hypernuclear physics such as the "coherent ΛN-ΣN coupling" as discussed intensively in theory.

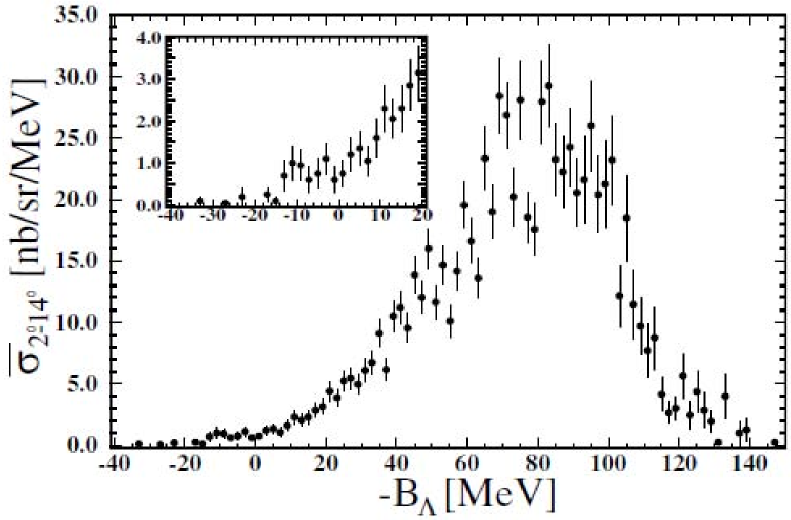

Figure 1: Excitation energy spectrum of the ${}^{10}_{\Lambda}$Li hypernucleus for the (π^-, K^+) reaction on a ^{10}B target from Ref.[21]. The inset shows closeup of the Λ bound region. The amount of possible background can be estimated from entries in the region $-B_\Lambda < -20MeV$, and is small.

3. Feedback to other fields, like astrophysics, for the detailed understanding of various phenomena of high density nuclear matter in a neutron star.

4. Study of the Λ-hypernucleus with a large neutron excess in connection with the nuclear physics near the neutron drip line, where so-called a "neutron halo" has been studied over years.

Details of the new fields of studies are described in the following sections.

1.2.1 Production of neutron-rich and exotic Λ-hypernuclei

Marjling pointed out that we may produce neutron-rich Λ-hypernuclei by the double charge-exchange (DCX) reactions, like the (K^-, π^+) reaction, and the neutron-rich hypernuclei could be quite exotic[23]. The DCX reactions on the ^{6}Li or ^{7}Li target will produce the ${}^6_\Lambda$H or ${}^7_\Lambda$H hypernucleus, which would be very exotic nucleus with a large neutron to proton ratio, N/Z=4 for ${}^6_\Lambda$H or N/Z=5 for ${}^7_\Lambda$H.

A possibility of a binding of the ${}^6_\Lambda$H, "hyper-heavy hydrogen", ground state was already discussed in detail theoretically by Akaishi, *et al.*[24] as seen in Fig.2. The ground state of the core nucleus, ^{5}H, is known as a broad resonance state ($E_X \sim 1.7MeV$) and is called "super-heavy hydrogen". The resonance state may be bound due to the attractive interaction between the Λ hyperon and the core nucleus. We may expect large structure change of the core nucleus beyond the neutron drip line by the addition of the Λ hyperon.

1.2.2 Study on two- and three-body interactions in Λ-hypernuclei

Since the mass difference between the Λ and Σ hyperons is small, $\delta M_{\Lambda\Sigma} \sim$80MeV/c^2, compared with that of the nucleon and Δ isobar, $\delta M_{N\Delta} \sim$290MeV/c^2. This situation makes the effect of the ΛN-ΣN channel-coupling quite important in the discussion of the hypernuclear level

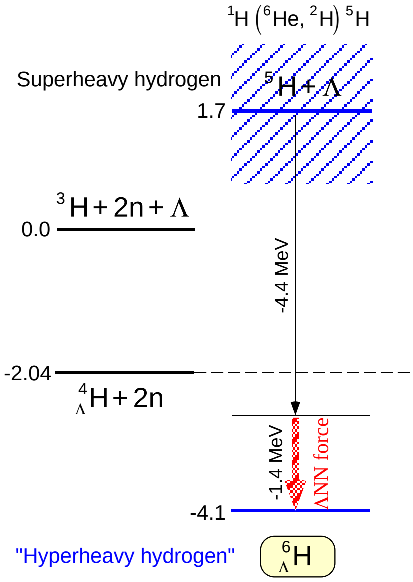

Figure 2: Formation of $^6_\Lambda$H, "hyper-heavy hydrogen". It has a resonance state of ^{5}H, "super-heavy hydrogen", as the nuclear core. The Λ binding energy is calculated to be rather large, $\sim$4.1 MeV, if the ΛN-ΣN coupling effect is included.

structure[25]. The strong ΛN-ΣN coupling introduce an additional effective two-body interaction between Λ and nucleon, and also may be a source of the tree-body interaction among the ΛNN subsystem in a Λ-hypernucleus.

Recently, Akaishi, *et al.*[26] solved the so called "under-binding problem" of the Λ separation energy in the $^4_\Lambda$He hypernucleus by introducing explicitly the ΛN-ΣN coupling in the hypernucleus known as "coherent ΛN-ΣN coupling", by their definition, in which nucleons remain in the ground state when converting Λ to Σ, leading all the nucleons to interact with Σ in an equal footing in order to convert Σ to Λ again. The "coherent ΛN-ΣN coupling" can be studied through the level structure of the neutron-rich Λ-hypernuclei and also observable by directly populating a Σ^- component in the Λ hypernuclear states by the (π^-, K^+) reaction.

1.2.3 Connection to astrophysics: ingredients of neutron stars

The knowledge obtained from this study will give a feed back not only to the nuclear physics but also to other fields like astrophysics. It has been intensively discussed that hyperons in a high-density nuclear matter in neutron stars play a significant role concerning the maximal mass of a neutron star, formation-scenario and a thermal and structural evolution of a neutron star and a black hole[27]. Namely, the presence of hyperons in a neutron star makes the Equation of State (EoS) much softer than that without hyperons. In particular, the role of Σ^- mixing in a neutron star is being intensively discussed in the present days because of a negative charge of Σ^-[28]. However, the mixing will particularly depend on the Σ^-N interaction.

Recently, we measured the inclusive (π^-, K^+) spectra on different medium to heavy nuclear targets in order to obtain the Σ^--nucleus optical potential which has not been well known[29]. The experimental spectrum of Si target was compared with a theoretical calculation based on the Distorted-Wave Impulse Approximation (DWIA) showed that a very strong repulsive Σ^--nucleus potential was needed to reproduce the observed spectral shape[30]. Then, Σ^--

hyperons may not appear in the neutron star for a repulsive Σ^-N interaction. On the other hand, Akaishi, *et al.* discussed recently that the "coherent ΛN-ΣN coupling" will enhance the Σ mixing in the neutron star matter and needs to be taken into account in such theoretical calculations. In a recent calculation by Shinmura, *et al.*[31], ΛN-ΣN mixing is found very significant, particularly, a large ΛN-Σ^0N mixing is reported. It would be interesting as well as a good feedback to those theoretical calculations if the "coherent ΛN-ΣN coupling" effect can be observed experimentally.

1.2.4 Study on Λ-hypernuclei with neutron halo

In the conventional nuclear physics, studies of neutron-rich nuclei near the neutron drip line have been done extensively over the years, and as a result so-called a "neutron skin" and a "neutron halo" have been discovered. The structures of such nuclei have revealed interesting phenomena regarding its size, properties of excited states and so on[32, 33]. It is also interesting and necessary to study such a neutron-rich nucleus containing a Λ hyperon, which may change properties of a halo nucleus. The structures of light Λ-hypernuclei with the neutron skin or halo were already discussed theoretically[34] and we may expect rich variations of the structures.

1.2.5 Reaction mechanism: one- or two-step mechanism ?

As we mentioned, we think the DCX reaction is one of promising reactions to investigate the neutron-rich Λ-hypernuclei, but the reaction mechanism is not well understood, yet. The DCX reaction changes two protons in a nucleus to a Λ hyperon and a neutron, pp→Λn, so a naive explanation of the reaction is the two-step process, such as:

$$\pi^- pp \to K^0 \Lambda p \to K^+ \Lambda n$$

$$\pi^- pp \to \pi^0 pn \to K^+ \Lambda n$$

A theoretical calculation based on the two-step mechanism has been made[35]. The calculation predicted the ${}^{10}\mathrm{B}(\pi^-, K^+){}^{10}_{\Lambda}\mathrm{Li}$ reaction cross section of 66.8 nb/sr at 1.05 GeV/c pion beam momentum. The predicted reaction cross section considerably larger than the experimental results, ∼10 nb/s. Another theoretical prediction was that the DCX reaction cross section from the two-step process had a maximum at around the 1.05 GeV/c beam momentum. The result reflected the fact that the single charge-exchange reactions, the (π^-, K^0), (π^-, π^0) and (π^0, K^+) reactions, involved in the two-step process had large cross sections around 1.05 GeV/c. However, the theoretical prediction had a conflict with the results from the KEK-PS-E521 experiment, in which the DCX cross section is larger at the 1.20 GeV/c beam momentum than at 1.05 GeV/c.

A model which may explain the beam momentum dependence of the DCX reaction cross section is the one-step mechanism through the ΛN-ΣN mixing. In the one-step mechanism, a Σ^- hyperon is produced by the DCX reaction, π^-p→$K^+\Sigma^-$. Since the Σ^- hyperon may be mixed with a Λ hyperon in a nucleus by the ΛN-ΣN mixing, "Λn"↔"Σ^-p", the Λ state may be excited directly by the one-step reaction. The DCX cross section by the one-step mechanism depends on the elementary $p(\pi^-, K^+)\Sigma^-$ reaction cross section and the degrees of the ΛN-ΣN mixing in the Λ-hypernucleus to be created. Since the $p(\pi^-, K^+)\Sigma^-$ reaction has a production threshold at around 1.035 GeV/c in pion beam momentum, the reaction cross section increase rapidly from 1.05 GeV/c to 1.20 GeV/c. The beam momentum dependence of the elementary $p(\pi^-, K^+)\Sigma^-$ reaction cross section may interpret the experimental DCX reaction cross sections. However, the absolute values of the cross sections estimated from the

Table 1: Six amplitudes in the non-mesonic weak decay process whose initial ΛN system is in relative S-states.

Initial	Final	Matrix element	Rate	I_f	Parity change
$^1S_0$	$^1S_0$	a	a^2	1	no
	$^3P_0$	$\frac{b}{2}(\sigma_1 - \sigma_2)q$	b^2	1	yes
$^3S_1$	$^3S_1$	c	c^2	0	no
	$^3D_1$	$\frac{d}{2\sqrt{2}}S_{12}(q)$	d^2	0	no
	$^1P_1$	$\frac{\sqrt{3}}{2}e(\sigma_1 - \sigma_2)q$	e^2	0	yes
	$^3P_1$	$\frac{\sqrt{6}}{4}f(\sigma_1 + \sigma_2)q$	f^2	1	yes

one-step mechanism depend on the degrees of the ΛN-ΣN mixing strongly, and a considerable amount of mixing is necessary to reproduce the experimental cross sections.

At this moment, we need much more experimental information on the DCX reaction to know the reaction mechanism. The study on the DCX reaction mechanism is also one of key issues for copious production of the neutron-rich Λ-hypernuclei.

1.3 Study on ΛN weak interaction

The study of the weak ΛN interaction has long history experimentally and theoretically. In recent years, precise measurements of branching ratios, decay widths and decay asymmetries became available from a series of experiments, and estimated values for these observables from different theoretical calculations were converged. However, explanations of the experimental values by the theoretical calculations are still controversial. The situation is described in the following sections.

Another long standing puzzle is the strong selection of ΔI=1/2 channels, so called "Δ=1/2 rule", which is necessary to explain the hyperon weak decays but difficult to be reproduced by any theoretical calculations. There are discussions that the "ΔI=1/2 rule" may be broken in the non-mesonic weak decay of Λ-hypernuclei, but no conclusion is obtained, yet.

1.3.1 Partial decay rates of non-mesonic weak decay

The matrix element of the non-mesonic weak decay can be classified into six amplitudes depending on spin, isospin and parity of the initial and final states as shown in Table 1 provided that the initial state is of relative S-wave[10]. Study of partial decay rates ($\Lambda n \to nn$ and $\Lambda p \to np$) can constrain magnitude of each amplitude in terms of isospin (I_f in Table 1) because the nn and the np pairs have different fractions of the isospin components. Phenomenological analysis of s-shell hypernuclei indicates the dominance of the amplitude f (isospin 1 final state)[10]. On the contrary, theoretical prediction based on the pion exchange model implies the dominance of the amplitude d (isospin 0 final state) which is reflecting the tensor part of the potential[36, 37]. This discrepancy had existed for a long time even though heavier mesons, like ρ/ω, K* and σ, are included in the calculations[38, 39].

Recently KEK-PS-E462[40] and E508[41] collaborations have been carried out in order to solve above discrepancy. In the experiments, all the decay particles were measured and the kinematics of the non-mesonic weak decay, a back-to-back emission of a NN pair, were reconstructed, in order to avoid the contribution due to the final state interaction and the $\Lambda NN \to NNN$ process. The branching ratios, $\Gamma(\Lambda n \to nn)/\Gamma(\Lambda p \to np)$, so-called np-ratio, were obtained from the experiments. The values were $0.45 \pm 0.11(stat) \pm 0.03(syst)$ for ${}^{5}_{\Lambda}$He[42] $0.51 \pm 0.13(stat) \pm 0.04(syst)$ for ${}^{12}_{\Lambda}$C[43, 44]. The experiments also tell us the importance of the effect due to the final state interaction and/or the $\Lambda NN \to NNN$ process. The E462 experiment found that the effect was about 30 % of the non-mesonic weak decay even for ${}^{5}_{\Lambda}$He. Therefore, the exclusive measurement with coincidence of all the decay particles is essential to determine the observables of the non-mesonic weak decay.

On the other hand, the most recent theoretical calculation shows that a constructive contribution of the kaon exchange makes the amplitudes f comparable to the amplitude d and the partial decay rates are now compatible with the recent experimental result, consequently[45].

1.3.2 Weak decay of polarized Λ-hypernuclei

The parity violation of the non-mesonic weak decay process provides us interesting quantity to investigate the spin-parity structure of the ΛN weak interaction. The quantity is the decay asymmetry parameter, which relates to the asymmetric emission of decay particle with respect to the Λ polarization[46]. The asymmetry is due to interference between parity conserving and violating amplitudes, and expressed in terms of the six amplitudes in Table 1 as follows:[47]

$$\alpha_p^{NM} = \frac{2\sqrt{3}Re[-ae^* + b(c - \sqrt{2}d)^* - f(\sqrt{2}c + d)^*]}{\{a^2 + b^2 + 3(c^2 + d^2 + e^2 + f^2)\}}. \tag{1}$$

As discussed in the previous section, the amplitudes f and d are considered to have large contributions to the non-mesonic decay widths, theoretically. Therefore, the asymmetry parameter is mainly determined by the last term in Eq.(1), $f(\sqrt{2}c + d)$, which is sensitive to the ${}^3S_1$ component in the initial ΛN state. However, there are other two terms, ae and $b(c - \sqrt{2}d)$, which come from interference between the initial ${}^1S_0$ and ${}^3S_1$ amplitudes. These two terms were ignored in old expression by Bando, *et al.*[48], since the ${}^1S_0$ states have no asymmetry by themselves. A calculation based on the direct quark-exchange model suggests the importance of the initial ${}^1S_0$ states[49]. Therefore, the reason of the importance of the decay asymmetry parameter is that the parameter is sensitive to the both initial states, ${}^1S_0$ and ${}^3S_1$, while the decay rates (except for the non-mesonic weak decay of ${}^{4}_{\Lambda}$H and ${}^{4}_{\Lambda}$He) is not affected so much by the ${}^1S_0$ initial state because of the large number of quantum states of the initial ${}^3S_1$ states.

Experimentally, a quite large value (-1.3 ± 0.4) of the asymmetry parameter was observed for the non-mesonic weak decay of the polarized ${}^{12}_{\Lambda}$C and ${}^{11}_{\Lambda}$B hypernuclei by using the ^{12}C(π^+, K^+) reaction (KEK-PS-E160)[50]. It suggested equal importance of the isospin 0 (d) and 1 (f) amplitudes and seemed to contradict to phenomenological analysis of branching ratio at that moment which suggested the dominance of the isospin 1 final state. However, we had an error of 40 % for the asymmetry parameter. It was far below the accuracy that was needed for the detailed comparison with theoretical calculation. We thus have carried out a new experiment where the asymmetric non-mesonic weak decay was observed from the decay of polarized ${}^{5}_{\Lambda}$He hypernucleus[51].

The E278 experiment was carried out at the K6 beamline of KEK-PS. The ^{6}Li$(\pi^+, K^+p){}^{5}_{\Lambda}$He reaction at $P_\pi = 1.05$ GeV/c was used to produce polarized ${}^{5}_{\Lambda}$He. The experiment demonstrated that the polarized ${}^{5}_{\Lambda}$He hypernucleus was really produced by the (π^+, K^+) reaction[52]. The degrees of polarization was determined experimentally from the decay asymmetry of the mesonic decay of the hypernucleus. The large asymmetry parameter and the large branching ratio of the ${}^{5}_{\Lambda}$He mesonic decay were essential for the precise measurement of the degrees of the polarization of the Λ-hyperon in the hypernucleus. The observed polarization was consistent with the DWIA calculation[53], which includes the Λ polarization in the elementary reaction, ^{6}Li$(\pi^+, K^+){}^{6}_{\Lambda}$Li, and the depolarization due to proton emission, ${}^{6}_{\Lambda}\text{Li} \to {}^{5}_{\Lambda}\text{He} + p$.

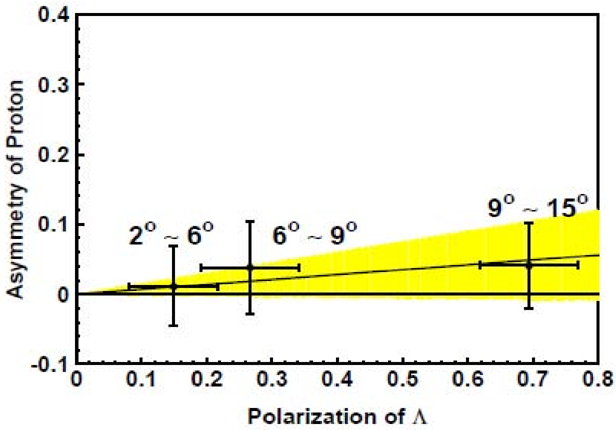

Figure 3: The plot shows the decay asymmetry of proton vs the polarization of Λ in the ${}^{5}_{\Lambda}$He non-mesonic weak decay. The tangent of the correlation between the proton asymmetry and the Λ polarization is a measure of the decay asymmetry parameter.

The asymmetry parameter of the non-mesonic weak decay derived from the Λ polarization and the proton asymmetry was $\alpha_p^{NM} = 0.24 \pm 0.22$[15]. The result showed that the asymmetry parameter of the non-mesonic weak decay had a positive sign and its magnitude was quite small compared to that obtained in the E160 experiment. One expected a contribution of the relative P-state in the initial ΛN system for the p-shell hypernuclei, ${}^{12}_{\Lambda}$C and ${}^{11}_{\Lambda}$B, although most of the decay rate came from the initial S-state according to Ref.[54]. The theoretical calculations based on the meson-exchange model estimated the asymmetry parameter to be around -0.7 independently of hypernuclear species. So, the theory preferred the results of the E160 experiment rather than the E278 experiment.

Recently, the E462 experiment[40] carried out with using same reaction in the E278 experiment. The result suggests that the asymmetry parameter of the non-mesonic weak decay of the ${}^{5}_{\Lambda}$He hypernucleus is quite small and consistent with the E278 experiment as shown in Fig.3[55]. Besides, a preliminary analysis of the E508 experiment shows that the asymmetry parameters for the ${}^{12}_{\Lambda}$C and ${}^{11}_{\Lambda}$B hypernuclei are also as small as that of the ${}^{5}_{\Lambda}$He case, and contradicts the E160 result. Although, the definite conclusion can not be derived from the E508 experiment due to the difficulty in the determination of the hypernuclear polarization, the experiments suggest the asymmetry parameter for the non-mesonic weak decay is small for the p-shell hypernuclei.

So, currently we believe the values of the asymmetry parameter of the non-mesonic weak decays are small, close to 0, for both s-shell and p-shell Λ-hypernuclei, while the theory estimates it to be around -0.7.

1.3.3 Importance of the precise measurement of A=4, 5 hypernuclei

As discussed above, recent experimental results on the branching ratios become compatible with the theoretical estimations. However, no theory can not explain the values of the asymmetry parameter. The branching ratios (or partial decay rates) are mainly determined by the initial ${}^3S_1$ amplitudes, because the number of quantum states of the initial ${}^3S_1$ states are three times larger than that of the ${}^1S_0$ states. However, the asymmetry parameter is determined by the interference not only among the initial ${}^3S_1$ states but also between the initial ${}^3S_1$ and ${}^1S_0$ states.

Table 2: Allowed initial states of the initial ΛN pair in the A=4, 5 hypernuclei.

Hypernucleus	$\Lambda n \to nn$	$\Lambda p \to np$
${}^4_\Lambda$H	${}^1S_0$, ${}^3S_1$	${}^1S_0$
${}^4_\Lambda$He	${}^1S_0$	${}^1S_0$, ${}^3S_1$
${}^5_\Lambda$He	${}^1S_0$, ${}^3S_1$	${}^1S_0$, ${}^3S_1$

Therefore the exclusive measurement of the initial ${}^1S_0$ contribution is essential to understand the branching ratio and the decay asymmetry of the non-mesonic weak decay at the same time.

Table 2 shows allowed initial states of the non-mesonic weak decay for the A=4, 5 hypernuclei. Since a pp (nn) pair in ${}^4_\Lambda$He (${}^4_\Lambda$H) forms 0^+ state, and Λ and another n (p) couples to 0^+ to form overall 0^+ spin-parity of the hypernuclear ground state, then the $\Lambda n \to nn$ ($\Lambda p \to np$) decay for the ${}^4_\Lambda$He (${}^4_\Lambda$H) hypernucleus starts only from the ${}^1S_0$ states. One can determine directly the initial ${}^1S_0$ amplitudes with measurements of these decay modes.

There is another interest in the measurement of the ${}^1S_0$ amplitudes. If the "ΔI=1/2" rule is hold in the non-mesonic weak decay, the ratio of above two decay modes, $\Lambda p \to np$ in ${}^4_\Lambda$H and $\Lambda n \to nn$ in ${}^4_\Lambda$He, is expected to be 1:2, while if ΔI=3/2 amplitude dominates we found the ratio to be 2:1. The precise measurements of these decay modes can provide an opportunity to test the ΔI=1/2 rule in the non-mesonic weak decay. So far, the ΔI=1/2 rule have been proposed only from the experimental results of the free decays of hyperons and mesons. Another test of the contribution of the ΔI=3/2 amplitude has been discussed by Schumacher[56], in which experimental values of $\Gamma_n/\Gamma_p({}^4_\Lambda\mathrm{He})$, $\Gamma_n/\Gamma_p({}^5_\Lambda\mathrm{He})$ and $\Gamma_{NM}({}^4_\Lambda\mathrm{He})/\Gamma_{NM}({}^5_\Lambda\mathrm{He})$ have been used. Experimental data on the non-mesonic weak decays of the ${}^4_\Lambda$He and ${}^4_\Lambda$H hypernuclei are also important for such test.

The measurement of the asymmetry parameter for ${}^5_\Lambda$He is also important, since we can not determine each amplitude of a specific initial state only from the measurement of the decay rate. Before the KEK-PS-E462 experiment, only the decay protons were measured to derive the asymmetry parameter. As mentioned above, the effect of the final state interaction is considerably large even for ${}^5_\Lambda$He. Recently, E462 reported the asymmetry parameter of ${}^5_\Lambda$He by a coincidence measurement of a pair of proton and neutron in the back-to-back kinematics[55]. So, we already have some information on the decay amplitudes from the asymmetry measurement which is complementary with information to be obtained from the study on the A=4 hypernuclei.

2 Our Strategy

2.1 Production of mirror and neutron-rich hypernuclei

In Sections 1.2 and 1.3, we mentioned on several key experiments to access to the open issues related with the ΛN strong and weak interactions in the Λ-hypernuclei. These experiments, of course, require high-precision measurements, and also require productions of mirror hypernuclei, ${}^{4}_{\Lambda}$H and ${}^{4}_{\Lambda}$He, and neutron-rich hypernuclei, for which production methods are not well established, yet. So, in this proposal, we wish to propose the establishment of methods to produce the mirror and neutron-rich hypernuclei by the *charge-exchange (CX) reactions*, and propose to investigate the open issues by the new spectroscopic tools.

2.2 Production of mirror hypernuclei

The mirror hypernuclei like ${}^{4}_{\Lambda}$H have ever been produced only as hyper-fragments. The production mechanism of the hyper-fragments is relatively complex compared with that of the hypernuclear production by the direct reactions, such as the (K^-, π^-) and (π^+, K^+) reactions. So, it is difficult to identify the formation of the mirror hypernuclei without the weak decay information. Since we wish to measure the weak decay process itself and investigate the decay channel with a tiny branching, the identification of the production of the mirror hypernuclei in the production reaction is essential. So, we have to use the direct reaction to produce the mirror hypernuclei.

The production and identification of the mirror hypernuclei with the direct reactions also have several difficulties if we use conventional experimental methods. The production of the mirror hypernuclei necessary to measure the (K^-, π^0) or (π^-, K^0) reaction.

If we use the (K^-, π^0) reaction, we need to measure 2γ from the π^0 decay. The 2γ detection and the π^0 reconstruction with an energy resolution of a few MeV level in the energy region of 1 GeV are quite difficult. A challenge of the measurement of the $(K^-_{Stopped}, \pi^0)$ reaction has ever made at BNL-AGS[57]. The experiment used a large volume of photon detectors, Neutral Meson Spectrometer (NMS), and achieved a few MeV (FWHM) resolution for π^0 of $\sim$250 MeV in energy. In the experiment, various kinamatical cuts have been made to achieve the good energy resolution, and it resulted in a low detection efficiency. So, an extension of the method to the GeV energy π^0, which is necessary for our study, is quite difficult due to the deterioration of the energy resolution and the low efficiency.

Another option is the (π^-, K^0) reaction which needs a detection of a pair of charged pions from the K_S decay, $K_S \to \pi^+\pi^-$. The precise measurement of the momentum of the charger pions is possible, in principle, if we have a two-arm spectrometer with a good momentum resolution. So, we believe the (π^-, K^0) reaction is a solution for the method to produce and precisely identify the mirror hypernuclei. However, the acceptance of the K_S detection with such a two-arm spectrometer is usually considerably small compared with a single-arm spectrometer, and we need some idea to increase the rate of the hypernuclear production. An answer is a development of the high-intensity and high-resolution (HIHR) beamline (details will be discussed in Sec.2.4).

2.3 Production of neutron-rich hypernuclei

For the production of the neutron-rich hypernuclei, we believe, the double charge-exchange reactions (DCX), the (π^-, K^+) and (K^-, π^+) reactions, are the only tools available at this moment, and the feasibility of the (π^-, K^+) reaction was demonstrated in the KEK-PS-E521 experiment[21]. A practical problem is the tiny reaction cross section of the DCX reaction. As we mentioned in Sec.1.2, the cross section of the (π^-, K^+) reaction is roughly 10^{-3} of that of the (π^+, K^+) reaction.

The cross section of the hypernuclear production by the (K^-, π^+) reaction is not known, yet. If the ratio of the (K^-, π^+) and (K^-, π^-) reaction cross sections is in the same level of that for the (π, K) reaction, i.e., 10^{-3}, the (K^-, π^+) reaction is not so promising because the K^- beam intensity is still much smaller than the π^- beam intensity even at J-PARC 50 GeV PS.

We have to override the small cross section problem to get enough yields of the hypernuclear production for the systematic study of the neutron-rich hypernuclei. Also for this purpose, we propose the development of the high-intensity and high-resolution (HIHR) beamline and spectrometer system to override the difficulty.

2.4 High-intensity and high-resolution (HIHR) beamline

The HIHR beamline and spectrometer system was originally designed for high-resolution measurements. Since the thickness of the nuclear target is a major factor of the experimental energy resolution due to the multiple-scattering and the energy loss difference between beam and scattered particles, we have to use thin target to get a fine energy resolution of sub-MeV level. The thin target means less yield of the hypernuclear production, so the high-resolution beamline should be high-intensity at the same time to compensate for the small thickness of the target. This high-intensity nature needs a change of concepts of the beamline design. The new concepts are similar with that of EPICS at LAMPF[58], but the range of the accepted pion beam momentum is much higher[59].

Current design of the HIHR beamline may handle a pion beam with typically 10^9 particle/s and a good momentum resolution, $\Delta P/P \sim 10^{-4}$, can be achieved (for more details, see Appendix A). The beam intensity to be handled in the HIHR beamline is roughly 10^2 higher than that of the current maximum pion beam intensity, $\sim 10^7$/spill, so the new beamline will open a door to the new field of hypernuclear studies including our experimental proposals.

3 Proposed Experiments

Our strategy of the study on the Λ-hypernuclei is the development of the *charge-exchange reactions* to access to Λ-hypernuclei which have never been created copiously by direct reactions. To achieve the copious productions, the development of the *high-intensity and high-resolution (HIHR) beamline* is necessary. However, the development of the HIHR beamline takes time to optimize the design for J-PARC and also needs considerable amount of cost for a construction. So, we will take a two step approach for the study.

The 1st step, "phase 1", is a series of experiments which can be done with the infrastructures to be available at the Day-1. One of the "phase 1" experiments is the detailed study of the non-mesonic weak decay (NMWD) of the ${}^{4}_{\Lambda}$He hypernucleus for which we will use the conventional (π^+, K^+) reaction to produce the hypernucleus. The measurement of the NMWD for the ${}^{4}_{\Lambda}$He hypernucleus is a complementary process of that for the ${}^{4}_{\Lambda}$H hypernucleus, which can be created only by the charge-exchange reactions, the (π^-, K^0) reaction.

Another "phase 1" experiments is the study on the reaction mechanism of the formation of the neutron-rich hypernuclei by the double charge-exchange (DCX) reactions. The systematic study of the neutron-rich hypernuclei requires the construction of the HIHR beamline, but a study may be possible at the Day-1 on the reaction mechanism of the DCX reactions to know the optimum conditions of the production of the neutron-rich hypernuclei. It may affect also to the design of the HIHR beamline.

After the "phase 1" experiments, we wish to construct the HIHR beamline, and go the "phase 2". One of the "phase 2" experiments is the study on the NMWD of the ${}^{4}_{\Lambda}$H hypernucleus, which need the measurement of the (π^-, K^0) reaction to produce the hypernucleus. Another "phase 2 " experiment is the systematic study of the neutron-rich hypernuclei, and the HIHR beamline will provide a high production rate of the neutron-rich hypernuclei including very exotic objects like hypernuclei with the neutron halo.

3.1 Phase 1 experiments

As the "phase 1" experiment, here we describe the study on the NMWD of the ${}^{4}_{\Lambda}$He hypernuclei and the study on the reaction mechanism of the DCX reaction. In principle, these experiments need only infrastructures to be available at the J-PARC 50 GeV proton synchrotron facility at the Day-1. A beamtime summary of the "phase 1" experiments is shown in Table 3, and details are discussed in the following sections.

Table 3: Summary of beamtime requests for the "phase 1" experiments.

Subject	Beamtime request
Non-mesonic weak decay of ${}^{4}_{\Lambda}$He	2 weeks
Structure of the ${}^{10}_{\Lambda}$Li hypernuclei	2 weeks
The DCX reaction mechanism	1.5 weeks

3.1.1 Measurement of ${}^{4}_{\Lambda}$He non-mesonic weak decay

We use the ^{4}He(π^+, K^+) reaction with 1.1 GeV/c π^+ beam from the K1.8 beamline at the J-PARC 50 GeV PS to produce the ${}^{4}_{\Lambda}$He hypernucleus. Since the non spin-flip interaction is strong for the (π^+, K^+) reaction at the pion beam momentum, the reaction populates the 0^+

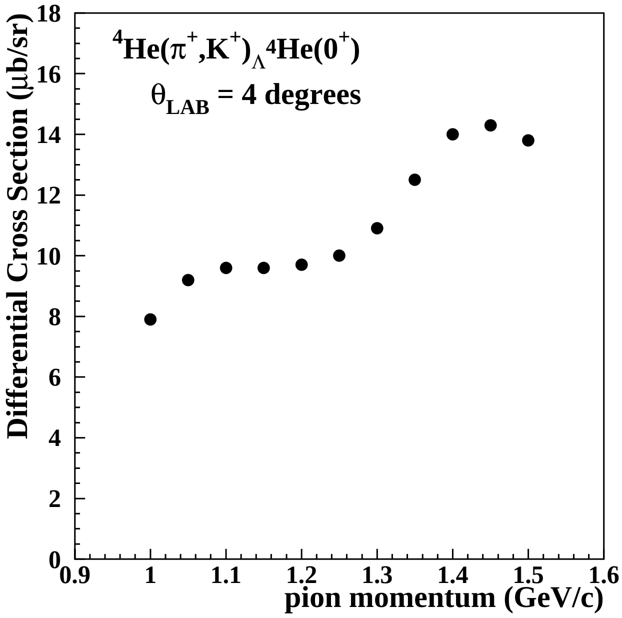

Figure 4: Theoretically estimated differential cross section of the $^4\mathrm{He}(\pi^+, K^+)^4_\Lambda\mathrm{He}(g.s., 0^+)$ reaction at θ_{LAB}=4° based on a DWIA calculation.

ground states of the $^4_\Lambda$He hypernucleus. Theoretical estimation of the reaction cross section was done based on a DWIA calculation[60], and the results is shown in Fig.4 as a function of the pion beam momentum. The Superconducting Kaon Spectrometer (SKS) is used to detect produced K^+ to achieve a large detection acceptance (∼100 msr) and good momentum resolution at the same time. The mass resolution of hypernuclei should be less than 2 MeV (FWHM), since the binding energy of the ground state of $^4_\Lambda$He is 2.4 MeV.

The decay particles are measured by the decay counter system which consists of drift chambers and stacks of plastic counters as shown in Fig.5. The drift chambers are for tracking of the charged particles. The plastic counters are used for determine the energy of the charged particles by measuring energy deposit and range. For the neutron, the energy is determined by measuring time of flight between the plastic counters and the timing counters surrounding the experimental target. The concept of the decay counter system is same with that used in a series of the experiment to measure the non-mesonic weak decay at KEK-PS, where we confirmed that the particle identification can be done well. The difference is only the coverage of the acceptance.

Table 4 shows basic parameters to estimate the yield of the non-mesonic weak decay events. The value of the pion beam momentum is set to relatively lower value, 1.1 GeV/c, because the SKS acceptance for the scattered kaon decreases as the increase of the beam energy and the momentum resolution also get worse. The rate of the $^4_\Lambda\mathrm{He}(0^+)$ production is estimated as follows:

$$Yield\ (^4_\Lambda\mathrm{He}(0^+)) = N_{Beam} \times \frac{N_{Target}}{4} \times N_A \times \frac{d\sigma}{d\Omega} \times \Omega_{SP} \times \varepsilon_{SP} \times \frac{Time}{T_{Cycle}} \qquad (2)$$

We expect 1.5 $^4_\Lambda\mathrm{He}(0^+)$/spill ∼ 38k $^4_\Lambda\mathrm{He}(0^+)$/day. By using parameters in Table 4, the event

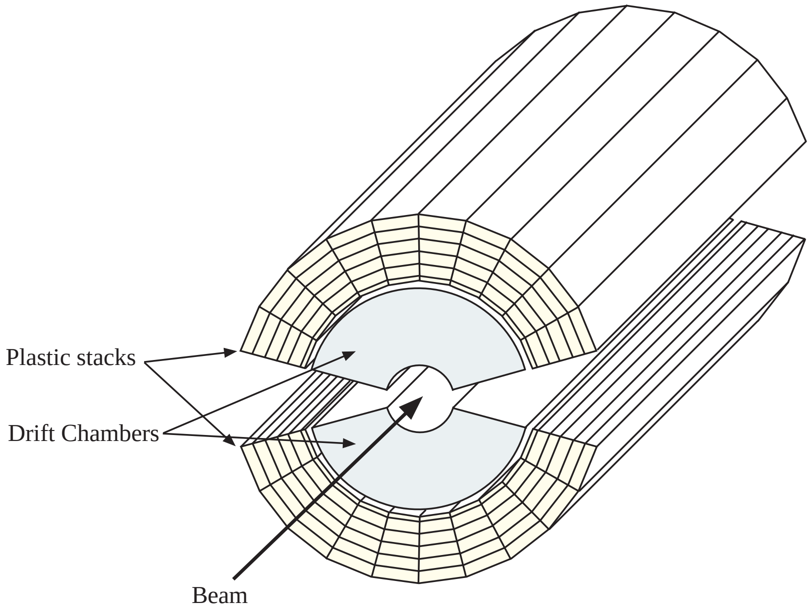

Figure 5: A Conceptual design of the decay counter system.

Table 4: Basic parameters for the measurement of the ${}^{4}_{\Lambda}$He non-mesonic weak decay events.

Parameters	Values	Parameter in Eqs.(2)–(4)
π^+ beam momentum	1.1 GeV/c	
π^+ beam intensity	1×10^7 /spill	N_{Beam}
PS acceleration cycle	3.4 sec	T_{Cycle}
^{4}He target thickness	2 g/cm^2	N_{Target}
Reaction cross section	10 μb/sr	$d\sigma/d\Omega$
Spectrometer solid angle	0.1 sr	Ω_{SP}
Spectrometer efficiency	0.5	ε_{SP}
Decay counter acceptance	0.5	a_{Decay}
Efficiency for decay protons	0.8	ε_p
Efficiency for decay neutrons	0.3	ε_n
Branching ratio of $\Gamma(\Lambda n \to nn)$	0.01	$BR(\Lambda n \to nn)$
Branching ratio of $\Gamma(\Lambda p \to np)$	0.1	$BR(\Lambda p \to np)$

Table 5: Basic parameters to estimate the ${}^4_\Lambda$He(0^+) yield by the (K^-, π^-) reaction.

Parameters	Values	Parameter in Eq.(2)
K^+ beam momentum	0.90 GeV/c	
K^+ beam intensity	3.6×10^5 /spill	N_{Beam}
PS acceleration cycle	3.4 sec	T_{Cycle}
^{4}He target thickness	$2\ g/cm^2$	N_{Target}
Reaction cross section	1.5 mb/sr	$d\sigma/d\Omega$
Spectrometer solid angle	0.02 sr	Ω_{SP}
Spectrometer efficiency	0.8	ε_{SP}

rates of the $\Lambda n \rightarrow nn$ and $\Lambda p \rightarrow np$ processes are estimated as follows:

$$Yield\ (\Lambda n \rightarrow nn) = Yield\ ({}^4_\Lambda\mathrm{He}(0^+)) \times BR(\Lambda n \rightarrow nn) \times (a_{Decay} \times \varepsilon_n)^2 \quad (3)$$

$$Yield\ (\Lambda p \rightarrow pn) = Yield\ ({}^4_\Lambda\mathrm{He}(0^+)) \times BR(\Lambda n \rightarrow pn) \times (a_{Decay} \times \varepsilon_n) \times (a_{Decay} \times \varepsilon_p) \quad (4)$$

We expect 120 events for the $\Lambda n \rightarrow nn$ decay and 3200 events for the $\Lambda p \rightarrow np$ decay in 2 weeks of beam time. We can achieve 9 % statistical error even for $\Lambda n \rightarrow nn$ decay process which we have to measure, while the existing data is $\Gamma(\Lambda p \rightarrow np)$=0.16±0.02 and $\Gamma(\Lambda n \rightarrow nn)$=0.01±0.05[14]. Please note that the current $\Gamma(\Lambda n \rightarrow nn)$ is just consistent with zero and a finite value is not obtained, yet. We believe we will be able to set a finite branching ratio of the $\Lambda n \rightarrow nn$ process in ${}^4_\Lambda$He hypernucleus for the first time.

In the discussions above, we plan the experiment at the K1.8 beamline with intense π^+ beams and SKS. Another option is an experiment with K^- beams at the K1.1 or the K1.8-BR beamline. The parameters necessary to design the experiment are listed in Table 5. The beam intensity estimation assumes the PS operation at 30 GeV, the primary proton beam intensity of 9 μA, and 0.9 GeV/c operation of the beamline. The SPES-2 spectrometer is used and the reaction cross section comes from the DWIA calculation[60]. Figure 6 (a) shows the theoretical differential cross section as a function of kaon beam momentum. Since the kaon beam intensity strongly depends on the beam momentum, the product of the differential cross section and the kaon beam intensity, which is a measure of yield, is also plotted in Fig. 6 (b). The value of the product in (b) for the 0.9 GeV/c beam momentum is not the maximum value (at around 1.1 GeV/c), but the beam momentum is limited by the maximum magnetic field of the SPES-2 spectrometer.

Event rate estimation results in ~66k ${}^4_\Lambda$He(0^+)/day. Although the rate is higher than the rate by the (π^+, K^+) reaction, we think the (K^-, π^-) reaction option at the K1.1 or K1.8-BR beamline has much larger ambiguity than the experiment at K1.8, e.g., the beamline construction, the K^- beam intensity at the early stage of the J-PARC operation, K^- decay backgrounds, etc.

3.1.2 Systematic study on reaction mechanism of DCX reaction

We also propose another experiment as the phase 1 experiment, a systematic study on the double charge-exchange (DCX) reaction on limited number of nuclear targets. The nuclear targets we use are ^{10}B and ^{12}C targets. We use the K1.8 beamline for the (π^-, K^+) reaction measurement, where 1.05 GeV/c and 1.20 GeV/c π^- beams are available. For the K^+ detection, SKS is used. The large acceptance together with good energy resolution of SKS is quite suitable for this kind of experiment where the production cross section is very small.

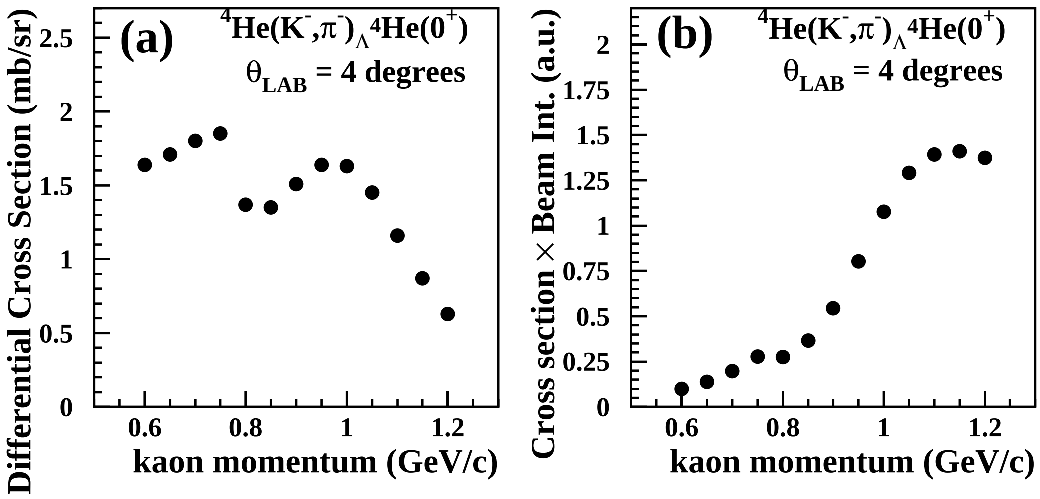

Figure 6: (a) Theoretically estimated differential cross section of the $^4\mathrm{He}(K^-,\pi^-)^4_\Lambda\mathrm{He}(g.s.,0^+)$ reaction at θ_{LAB}=4° based on a DWIA calculation, and (b) the product of the differential cross section and the kaon beam intensity.

Table 6: Basic parameters for the $^{10}_{\Lambda}$Li hypernucleus production.

Parameters	Values	Parameter in Eq.(5)
π^+ beam momentum	1.20 GeV/c	
π^+ beam intensity	1×10^7 /spill	N_{Beam}
PS acceleration cycle	3.4 sec	T_{Cycle}
^{10}B target thickness	3.5 g/cm^2	N_{Target}
Reaction cross section	10 nb/sr	$d\sigma/d\Omega$
Spectrometer solid angle	0.1 sr	Ω_{SP}
Spectrometer efficiency	0.5	ε_{SP}

The values of the production differential cross sections of the neutron-rich $^{10}_{\Lambda}$Li hypernucleus have been obtained from previous experiment[21], 5.8 ± 2.2 nb/sr at 1.05 GeV/c and 11.3 ± 1.9 nb/sr at 1.20 GeV/c. The event rate of the $^{10}_{\Lambda}$Li hypernucleus production at 1.20 GeV/c beam momentum is estimated from the differential cross section experimentally obtained together with other experimental parameters in Table 6 as follows:

$$Yield\ (^{10}_{\Lambda}\mathrm{Li}) = N_{Beam} \times \frac{N_{Target}}{10} \times N_A \times \frac{d\sigma}{d\Omega} \times \Omega_{SP} \times \varepsilon_{SP} \times \frac{Time}{T_{Cycle}} \qquad (5)$$

Then, by the above formula, we can expect about 370 events in 2 weeks of beamtime. This yield is roughly one order of magnitude larger compared with the yield in the previous experiment ($\sim$ 47 events). The larger yield makes us possible to discuss the neutron-rich hypernuclear level structure in more detail.

Together with the higher statistics measurement of the $^{10}_{\Lambda}$Li hypernucleus production at 1.20 GeV/c, we propose to make following measurements to understand the reaction mechanism of the DCX reaction which is important to discuss the optimum condition of the neutron-rich hypernuclei production:

Table 7: Beamtime necessary for the measurements and estimation of yields. No experimental information is available for the DCX reaction on the ^{12}C target, so far. So, these numbers are guesses from the ^{10}B target case. For more details, see text.

Hypernucleus	Beam momentum	Time necessary	Estimated yield	Subject
$^{10}_{\Lambda}$Li	1.20 GeV/c	2 weeks	370	$^{10}_{\Lambda}$Li structure
$^{10}_{\Lambda}$Li	1.05 GeV/c	0.5 week	~60	beam mom. dep.
$^{12}_{\Lambda}$Be	1.20 GeV/c	0.5 week	< 100	target dep.
$^{12}_{\Lambda}$Be	1.05 GeV/c	0.5 week	< 100	target dep.

1. Production of the $^{10}_{\Lambda}$Li hypernucleus also at the 1.05 GeV/c beam momentum. The production cross section seems to be smaller than that at the 1.20 GeV/c beam momentum by a factor of 2, while a theoretical calculation based on the two-step mechanism expects a larger production cross section.

2. Production of the $^{12}_{\Lambda}$Be hypernucleus with a ^{12}C target. The neutron $p_{3/2}$ orbit is closed for the ^{12}C target, while the ^{10}B target has a hole in the shell-model orbit. The difference may affect to both the two-step and the one-step mechanisms, and presumably the shell close decreases the cross section of the DCX reaction for the ^{12}C target. The degrees of the cross section change and its beam momentum dependence may give us information on the reaction mechanism. So, we propose to make measurements at the 1.05 GeV/c and 1.20 GeV/c beam momenta.

The beamtime for the additional study on the DCX reaction mechanism may be relatively short since we will not discuss details of the hypernuclear structure for the $^{12}_{\Lambda}$Be hypernucleus. Beamtime necessary for the measurements are listed in Table 7. A short energy and yield calibration runs with the ^{12}C target and the (π^+, K^+) setting are also necessary.

3.2 Phase 2 experiments

As the "phase 2" experiment, here we describe the detailed study on the non-mesonic weak decay of the $^{4}_{\Lambda}$H hypernucleus and the systematic study on the neutron-rich hypernuclei. These experiments have to wait the construction of the HIHR beamline.

In the following, we discuss the event rates in the "phase 2" experiments, but these numbers may have large ambiguity due to the performance of the HIHR beamline, the tolerable maximum count rate of the decay counter system, the mechanism of the DCX reaction, etc. More realistic estimation can be made after the construction of the HIHR beamline and the studies in the "phase 1".

3.2.1 Measurement of $^{4}_{\Lambda}$H non-mesonic weak decay

To produce $^{4}_{\Lambda}$H hypernucleus, we need to use single charge-exchange reactions. Here we propose to use the (π^-, K^0) reaction. Since the ^{4}He$(\pi^-, K^0)^{4}_{\Lambda}$H and ^{4}He$(\pi^+, K^+)^{4}_{\Lambda}$He reactions are isospin symmetric reactions each other, we can use the cross sections in Fig.4 as inputs in the following yield estimations.

The most significant difference between the (π^+, K^+) and the (π^-, K^0) reactions is the detection of the K^0 particle. Since K^0 usually can be detected as K_S and K_S decays mainly to a $\pi^+\pi^-$ (68.95%) or $2\pi^0$ (31.05%) pair, the detection efficiency of K^0 is much smaller

Table 8: Basic parameters for the measurement of the ${}^{4}_{\Lambda}$H NMWD events.

Parameters	Values	Parameter in Eqs.(6)
π^+ beam momentum	1.1 GeV/c	
π^+ beam intensity	1×10^9 /spill	N_{Beam}
PS acceleration cycle	3.4 sec	T_{Cycle}
^{4}He target thickness	1 g/cm^2	N_{Target}
Reaction cross section	10 μb/sr	$d\sigma/d\Omega$
Spectrometer solid angle	0.02 sr	Ω_{SP}
Spectrometer efficiency	0.03	ε_{SP}
Decay counter acceptance	0.5	a_{Decay}
Efficiency for decay protons	0.8	ε_p
Efficiency for decay neutrons	0.3	ε_n
Branching ratio of $\Gamma(\Lambda n \to nn)$	0.1	$BR(\Lambda n \to nn)$
Branching ratio of $\Gamma(\Lambda p \to np)$	0.01	$BR(\Lambda p \to np)$

than that of K^+. To override the difficulty of the small efficiency, we propose to use the high-intensity and high-resolution (HIHR) beamline and spectrometer. We can obtain beam intensity up to 10^9 π^-/spill at J-PARC. The binding energy of the ground state of ${}^{4}_{\Lambda}$H is 2 MeV. The spectrometer have to have a better energy resolution of 1.5 MeV (FWHM). The HIHR beamline and spectrometer system has enough resolution for the study. Based on the use of the HIHR beamline and experimental parameters listed in Table 8, we estimate the yield of the ${}^{4}_{\Lambda}$H hypernuclei as follows:

$$Yield\ ({}^{4}_{\Lambda}\mathrm{H}) = N_{Beam} \times \frac{N_{Target}}{4} \times N_A \times \frac{d\sigma}{d\Omega} \times \Omega_{SP} \times \varepsilon_{SP} \times \frac{Time}{T_{Cycle}} \tag{6}$$

In Table 8, the spectrometer acceptance ε_{SP} includes the decay branching ratio of K^0 ($K^0 \to K_S \to \pi^+\pi^-$; 34.5%) and the efficiency of the detection of the $\pi^+\pi^-$ pair.

We expect a production of $\sim$23k ${}^{4}_{\Lambda}$H/day. Then, we expect roughly 360 events for the $\Lambda n \to nn$ decay and 260 events for $\Lambda p \to np$ in a week. We can achieve 6 % statistical error even for $\Lambda p \to np$ which we have to measure, while we have only the decay rate of the non-mesonic weak decay ($\Gamma_{NM} = 0.17 \pm 0.11$) so far[14].

3.2.2 Systematic study on structure of neutron-rich hypernuclei

The HIHR beamline and spectrometer system is quite powerful also for the study of the neutron-rich hypernuclei with the DCX reaction. As listed in Table 8, we can expect pion beam intensity of 10^9 π^-/spill. The cross section of 10 nb/sr level corresponds to the event rate of $\sim$1000/day for the neutron-rich hypernuclei productions (spectrometer solid angle 0.04 sr is assumed). The high yield makes a systematic study of the neutron-rich hypernuclei possible, and makes a room to use much thinner nuclear targets to obtain a higher energy resolution which is essential for the spectroscopic study.

One of interesting hypernuclei to be studied in the "phase 2" is the exotic hypernucleus like ${}^{6}_{\Lambda}$H or ${}^{7}_{\Lambda}$H. The binding energy of such exotic hypernucleus is expected to be small, sub-MeV level, so the good resolution of the HIHR beamline and spectrometer system is quite powerful to separate the loosely bound state from the large quasi-free Λ production background.

4 Time Schedule and Cost Estimation

4.1 Phase 1 experiments

As already mentioned, the "phase 1" experiments use infrastructures, detectors, etc. to be available at the Day-1.

4.1.1 K1.8 beamline

The design of the K1.8 beamline has been finished, the preparation for the construction is proceeding, and the beamline will be ready at the Day-1. The beamline was designed to provide intense high-momentum kaon beams. The beamline provides also intense pion beams up to around $10^7\pi$/spill. The maximum beam intensity of the pion beams is limited by the single-rate of the beamline detectors if we use conventional tracking detectors like MWPC. The conventional beamline tracking detectors is now under designing and will be prepared by the KEK group.

The maximum beam intensity may be improved by a use of new techniques to handle the high counting rate. Developments of such new tracking detectors may be possible, if necessary, at the Osaka Univ. and Osaka Electrocommunications Univ. groups before the Day-1.

4.1.2 Spectrometer

We are planning to use the Superconducting Kaon Spectrometer (SKS) which has been used at the K6 beamline of KEK-PS. The spectrometer will be transfered to J-PARC 50 GeV PS and will be ready after several upgrades in the cryogenic system by the KEK group.

Another option may be the use of the SPES-2 spectrometer at the K1.8-BR (or K1.1) beamline. The SPES-2 spectrometer is now kept at the KEK-PS experimental facility and need a maintenance of the magnet itself for the use. The maintenance cost is not estimated, yet. A half of the tracking chamber has been constructed already, and Osaka group can construct another half, if necessary. The K1.8-BR beamline shares the upstream part with the K1.8 beamline and the downstream part will be constructed by the RIKEN and KEK groups because the K1.8-BR beamline is necessary also for other experimental proposals of J-PARC.

4.1.3 Target and decay counter system

The solid targets, ^{10}B and C, exist. We also need liquid ^{4}He target. A liquid ^{4}He target (cryostat) already exists at KEK-PS (property of the RIKEN group). We believe, the target can be used for our experiment with minor modifications.

We are planning to construct a general purpose decay counter system for several experiments at J-PARC under the collaboration of RIKEN, Osaka Univ., Osaka Electrocommunications Univ. and Kyoto Univ., and the KAKENHI budget is available for the construction. The design of the decay counter will be made in the fiscal year 2006, and will be ready before the Day-1. The design may be different from the conceptual design shown in Fig.5, but we are discussing to achieve required performances for experiments we are proposing.

4.2 Phase 2 experiments

To go to "phase 2", we need to construct the high-intensity and high-resolution pion beamline and spectrometer system. Since the beamline has no budget support at present, the time schedule of the "phase 2" is relatively unclear. However, we will make refinements of the beamline and spectrometer designs.

4.2.1 HIHR beamline

The basic design of the high-intensity and high-resolution beamline has been finished. The current design of the beamline fits into the experimental hall of J-PARC 50 GeV PS facility. Some further refinements, e.g., cost-reductions, size-reductions and magnet-recycles, will be made by a collaboration of the KEK and Osaka Univ. groups.

4.2.2 K^0 spectrometer

For the production of the ${}^{4}_{\Lambda}$H hypernucleus, we need K^0 spectrometer to measure the (π^-, K^0) reaction. A conceptual design of the spectrometer is in progress as a two-arm magnetic spectrometer by the Osaka group. Tracking detectors for the spectrometer may be prepared by the KAKENHI budged. The magnet itself does not exist, so we have to consider magnet-recycles or another source of budget for the magnet fabrication.

4.2.3 Target and decay counter system

The liquid ^{4}He target prepared in the "phase 1" can be used also in the "phase 2". Other nuclear targets are ready or easy to prepare. The decay counter system to be constructed for the "phase 1" experiments will have enough performances to be used in the "phase 2" experiments.

A High-Resolution GeV-Pion Beam line

The main proton synchrotron of J-PARC will deliver a high-power beam of 50 GeV and 15 μA. By taking advantage of the low-emittance primary beam, a *High-Intensity and High-Resolution (HIHR) GeV-Pion Beam Line* can be designed. The beam line will provide a pion intensity as high as 10^9 per second and a momentum resolution as good as 10^{-4}, which are respectively 1000-times more and 10-times better than those realized at K6 of the KEK 12-GeV PS [61]

The present beam-line facility will enable us to increase the production rate of hypernuclei drastically, and will provide us a so-called hypernuclear factory with the (π, K^+) reaction. The (π, K^+) reaction has unique features; 1) it favors to populate stretched states, 2) can produce polarized hypernuclei, and 3) is a background-free reaction. The (π, K^+) reaction plays a complementary role on the hypernuclear study to the (K^-, π) reaction. Thus, the pion beam line should be constructed. Utilizing the present facility, next-generation hypernuclear studies with high precision will be proceeded at J-PARC, where *high resolution, high statistics, and high sensitivity* will be key issues.

A layout of the proposed beam line is illustrated in Fig.7, together with a kaon spectrometer. The beam line consists of two halves. The first half is from PP to MS and for separating pions

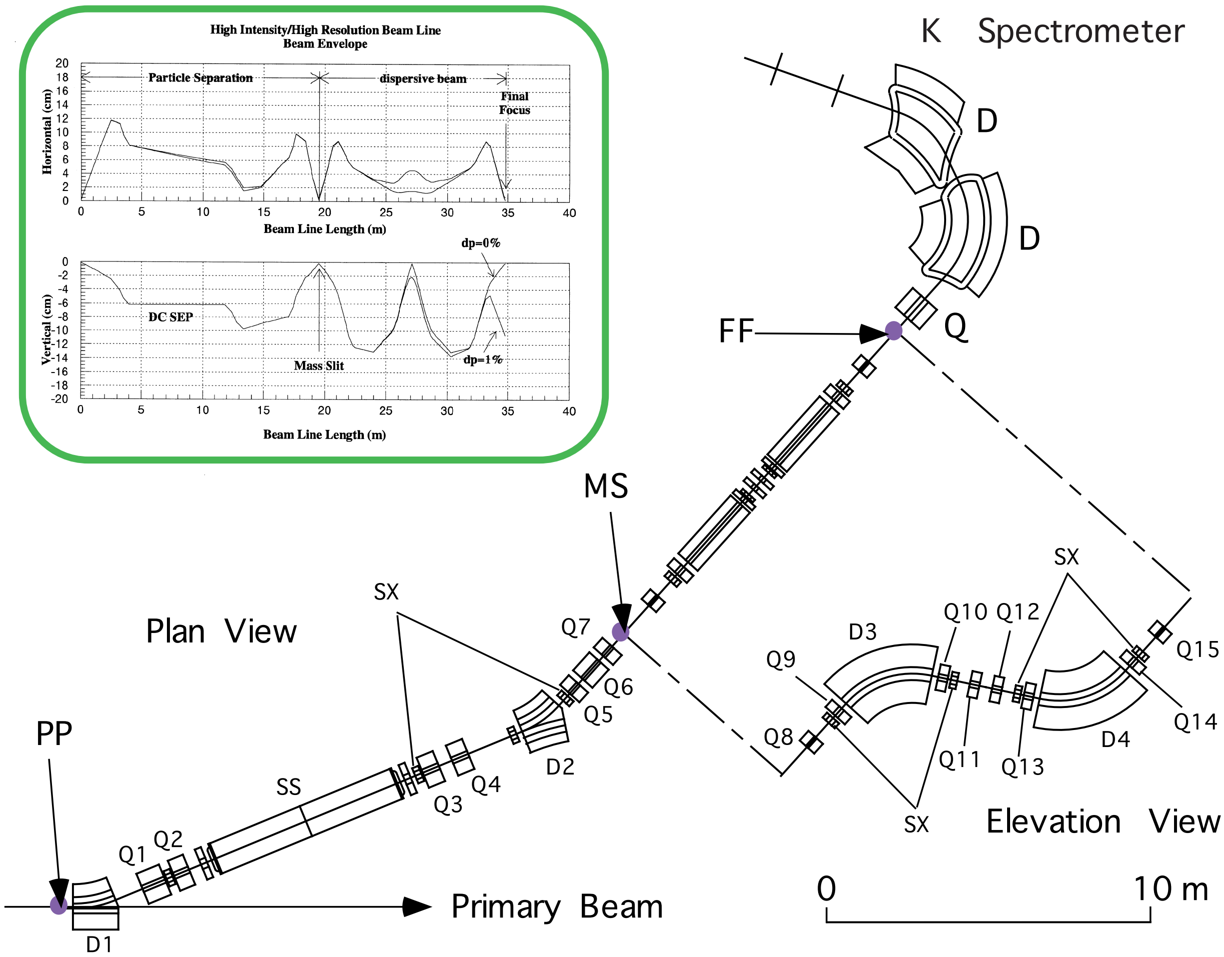

Figure 7: Layout of high-intensity and high-resolution pion beam line and kaon spectrometer.

from the other secondary particles with an electrostatic separator. The first part is so called "K1.8-BR" beam-line and will be constructed as the upstream part of the "K1.8" beam-line.

Since no tracking devices are available, due to the high counting rate, the beam momentum must be determined by measuring the reaction point where the beam position is strongly correlated with its momentum. Thus, the second half is from MS to FF and for making the beam dispersive vertically at FF. The dispersion and vertical magnification at FF are to be $\sim$10cm/% and -0.4, respectively. A momentum resolution of 10^{-4} can be achieved when the source size (production target) is smaller than 2.5mm.

The total length and acceptance of the beam line are 35m and 4msr·%. According to the Sanford-Wang formula[62] the π^+intensity is estimated to be more than 10^9 per second with a platinum production target 6cm long.

The kaon spectrometer in the figure is designed to be a resolution as good as 10^{-4} to match with the pion beam line. This is obviously optimized for the resolution, compromising with the acceptance and kaon survival rate. The specifications of the kaon spectrometer should be changed, if necessary, so that the resolution, acceptance, maximum central momentum, total length, cost, and so on, will have to meet experimental requests. The design concept of the kaon spectrometer is summarized as follows.

1. The kaon momentum is determined by the hit position at the focal plane. The resolution is almost determined by the horizontal beam size at the experimental target.

2. The vertical vertex point can be reconstructed from the vertical position and divergence at the focal plane. The vertex resolution of less than 1mm is thus required so that the beam momentum resolution is to be 10^{-4}, which is predominantly determined by the primary beam size at the production target.

3. Satisfying items 1 and 2, we could remove any vertex detectors at around the target, where the counting rate is expected to be too high to drive counters.

We could design a kaon spectrometer to meet above conditions. The horizontal magnification and dispersion are -0.851 and 8.327 cm/%, respectively. The vertical magnification ($R33$) is -3.08. Since the spectrometer has a vertical focus, the vertex resolution is determined by $Y_O = Y_I/R33 \sim 0.5\text{mm}/3.08 \sim 0.16\text{mm} << 1\text{mm}$, where Y_O and Y_I represent the vertex resolution (object size) and position resolution (image size) at the focal plane, respectively.

Specifications of the pion beam line and kaon spectrometer are summarized in Table 9.

Table 9: Specifications of the pion beam line and kaon spectrometer. [a] Corrections for higher order aberrations are required.

	π Beam Line	K Spectrometer
Max. Central Momentum (GeV/c)	1.5	1.5
Total Length (m)	34.738	12.4
Horizontal Acceptance (mrad)	±50	±100
Vertical Acceptance (mrad)	±10	±40
Momentum acceptance (%)	±1	±5
Horizontal Magnification	0.773	-0.851
Vertical Magnification	-0.409	-3.084
Dispersion (cm/%)	10.614	8.327
Momentum Resolution ($\Delta P/P$)	10^{-4}	10^{-4} [a]

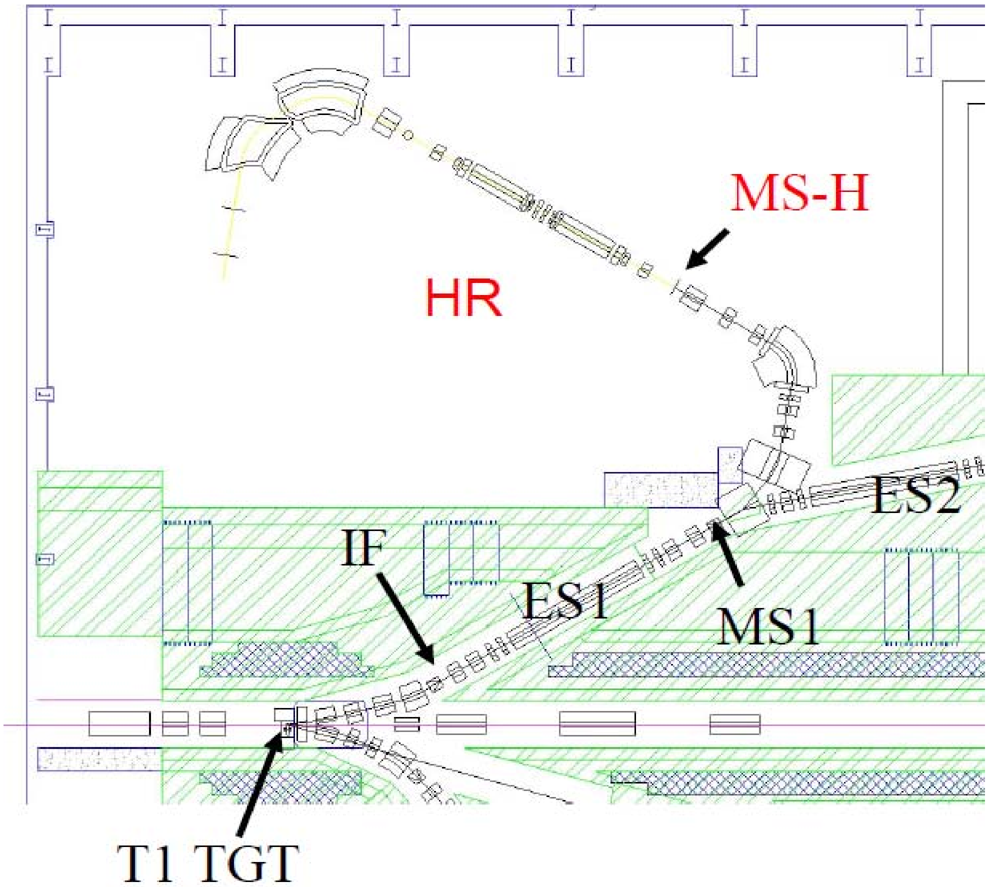

Figure 8: Layout of high-intensity and high-resolution pion beam line fitted to the current floor plan of the experimental hall.

An updated layout of the high-intensity and high-resolution beamline and kaon spectrometer fitted to current floor plan of the experimental hall is shown in Fig.8.

References

[1] M. Danysz and J. Pniewski, Bull. Acad. Pol. Sci. III **1** (1953) 42; M. Danysz and J. Pniewski, Phil. Mag. **44** (1953) 348.

[2] P.H. Pile, *et al.*, Phys. Rev. Lett. **66** (1991) 2585.

[3] T. Hasegawa, *et al.*, Phys. Rev. C **53** (1996) 1210.

[4] W. Brückner, *et al.*, Phys. Lett. B **79** (1978) 157.

[5] A. Bouyssy, Phys. Lett. B **84** (1979) 41.

[6] R.E. Chrien, *et al.*, Phys. Lett. B **89** (1979) 31.

[7] S. Ajimura, *et al.*, AGS-E929 Collaboration, Phys. Rev. Lett. **86** (2001) 4255.

[8] H. Tamura, *et al.*, Phys. Rev. Lett. **84** (2000) 5963.

[9] H. Akikawa, *et al.*, Phys. Rev. Lett. **88** (2002) 082501.

[10] M.M. Block and R.H. Dalitz, Phys. Rev. Lett. **11** (1963) 96.

[11] R. Grace, *et al.*, Phys. Rev. Lett.**55** (1985) 1055.

[12] J.J. Szymanski, *et al.*, Phys. Rev. C **43** (1991) 849.

[13] H. Noumi, *et al.*, Phys. Rev. C **52** (1995) 2936.

[14] H. Outa, *et al.*, Nucl. Phys. A **639** (1998) 251c.

[15] S. Ajimura, *et al.*, Phys. Rev. Lett. **84** (2000) 4052.

[16] H. Park, *et al.*, Phys. Rev. C **61** (2000) 054004.

[17] K. Itonaga, T. Ueda and T. Motoba, Phys. Rev. C **65** (2002) 034617.

[18] K. Sasaki, M. Izaki and M. Oka, Phys. Rev. C **71** (2005) 035502.

[19] K. Kubota, *et al.*, Nucl. Phys. A **602** (1996) 327.

[20] M. Agnello, *et al.*, FINUDA Collaboration, Nucl. Phys. A **752** (2005) 139c.

[21] P.K. Saha, *et al.*, KEK-PS-E521 Collaboration, Phys. Rev. Lett. **94** (2005) 052502.

[22] K. Tanida, *et al.*, Phys. Rev. Lett. **86** (2001) 1982.

[23] L. Majling, Nucl. Phys. A **585** (1995) 211c.

[24] Y. Akaishi, *et al.*, Frascati Physics Series, Vol. XVI, pp. 59-74 (1999); private communication, 2001-2002.

[25] B.F. Gibson, A. Goldberg and M.S. Weiss, Phys. Rev. C **6** (1972) 741.

[26] Y. Akaishi, Khin Swe Myint, T. Harada and S. Shinmura ,Phys. Rev. Lett. **84** (2000) 3539.

[27] M. Prakash and J.U. Lattimen, Nucl. Phys. A **639** (1998) 433c.

[28] S. Balberg and A. Gal, Nucl. Phys. A **625** (1997) 435.

[29] P.K. Saha, PhD. thesis, Sokendai (KEK-Rep. 2001-17).

[30] H. Noumi, *et al.*, KEK-PS-E438 Collaboration, Phys. Rev. Lett. **89** (2002) 072301.

[31] S. Shinmura, Y. Akaishi and T. Harada, Prog. Theor. Phys. **65** (1981) 1290.

[32] I. Tanihata, *et al.*, Phys. Rev. Lett. **55** (1985) 2676.

[33] T. Kobayashi, *et al.*, Phys. Rev. Lett. **60** (1988) 2599.

[34] E. Hiyama, Few-Body Systems **34** (2004) 79.

[35] T.Yu. Tretyakova and D.E. Lanskoy, Nucl. Phys. A **691** (1001) 51c.

[36] B.H.J. McKellar and B.F. Gibson, Phys. Rev. C **30** (1984) 322.

[37] K. Takeuchi, H. Takaki and H. Bando, Prog. Theor. Phys. **73** (1985) 841.

[38] J. Dubach, Nucl. Phys. A **450** (1986) 71c.

[39] A. Parreño, A. Ramos, and C. Bennhold, Phys. Rev. C **56** (1997) 339, and references therein.

[40] H. Outa, *et al.*, KEK-PS E462 proposal.

[41] H. Bhang, *et al.*, KEK-PS E508 proposal.

[42] B.H. Kang, *et al.*, Phys. rev. Lett. bf 96 (2006) 062301.

[43] H. Outa, *et al.*, Nucl. Phys. A **754** (2005) 157c.

[44] M.J. Kim, *et al.*, nucl-ex/0601029 (2006).

[45] A. Parreño and A. Ramos, Phys. Rev. C **65** (2001) 015204.

[46] T. Kishimoto, KEK-Rep. **83-6** (1983) 51, unpublished.

[47] H. Nabetani, T. Ogaito, T. Sato and T. Kishimoto, Phys. Rev. C **60** (1999) 017001.

[48] H. Bando, T. Motoba and J. Zofka, Int. J. Mod. Phys. Vol. **5** (1990) 4021.

[49] K. Sasaki, T. Inoue and M. Oka, nucl-th/0204057 (2002).

[50] S. Ajimura, *et al.*, Phys. Lett. B **282** (1992) 293.

[51] T. Kishimoto, *et al.*, KEK-PS E278 proposal.

[52] S. Ajimura, *et al.*, Phys. Rev. Lett. **80** (1998) 3471.

[53] K. Itonaga, T. Motoba, O. Richter and M. Sotona, Phys. Rev. C **49** (1994) 1045.

[54] C. Bennhold and A. Ramos, Phys. Rev. C **45** (1992) 3017.

[55] T. Maruta, *et al.*, nucl-ex/0509016 (2005).

[56] R.A. Schumacher, Nucl. Phys. A **547** (1992) 143c.

[57] M.W. Ahmed, *et al.*, Phys. Rev. C **68** (2003) 064004.

[58] D.J. Lisca and L.B. Dauelsberg, IEEE Trans. on Nucl. Sci. **24** (1977) 1577.

[59] H. Noumi, Nucl. Phys. A **639** (1998) 121c.

[60] T. Harada, private communication, 2006.

[61] The K6-SKS spectrometer system has realized about 50 events of the $^{12}_{\Lambda}C$ production per hour with a graphite target 1.8g/cm^2 thick.

[62] J.R. Sanford and C.L. Wang, BNL 11279 and BNL 11479 (1967); C.L. Wang, Phys. Rev. Lett., **25**, 1068 (1970).